Imaging Diagnosis of Shoulder Girdle Fractures

9

Joseph S. Yu

9.1 Introduction

The shoulder is vulnerable to both direct and indirect trauma, and fractures and dislocations are relatively common [1]. The shoulder girdle refers to a complex region of the skeleton that consists of numerous muscular and osseous structures, several joints containing fibrocartilage and hyaline cartilage, and ligaments and tendons that attach and suspend the arm to the thorax allowing for maximum mobility of the upper extremity. Muscles act synergistically to optimize motion.

Evaluation of the shoulder typically begins with a radiographic inspection of the osseous structures and joints. There are limitations associated with the radiographic evaluation. Certain fractures are difficult to visualize unless specific projections are performed. Complex fractures or fracture-dislocation complexes often are difficult to characterize owing to displacement of osseous fragments. Multi-detector CT has enabled rapid and accurate assessment of osseous and articular injuries. Depiction in an infinite number of imaging planes and three-dimensional (3D) images has rendered CT an indispensable modality for assessment of acute shoulder trauma.

Ultrasound is not routinely utilized in patients presenting with shoulder fractures but it is a useful follow-up modality for assessing the rotator cuff, vascular structures, and fluid collections that may have developed as a result of acute trauma. MRI is preferred for shoulder instability, but in the setting of acute trauma its role is limited to depicting marrow edema that is associated with acute contusions and occult fractures as well as for patients presenting with significant soft-tissue injuries.

J. S. Yu (✉)
Department of Radiology, The Ohio State University Wexner Medical Center, Columbus, OH, USA
e-mail: joseph.yu@osumc.edu

9.2 Clavicle

9.2.1 Pertinent Imaging Findings

The clavicle is an S-shaped bone that is unique, functioning as an osseous connection between the arm and the trunk. It is therefore vulnerable to trauma especially in children and adolescents. It is one of the first bones to ossify, though the medial epiphysis does not fuse until the second decade of life. Radiographic examination typically includes an AP view and a 35- to 40-degree cephalad-angled projection called the *serendipity* view. Owing to the curved contour of the bone, the serendipity view offers better visualization of the clavicle in its entirety and the sternoclavicular joints. Medially, it is tubular with a broad head that articulates with the manubrium and the first rib. Laterally, the clavicle becomes flatter with a discoid end that forms a gliding synovial joint with the acromion process. The AP view allows ideal inspection of the middle-third of the bone while the Zanca view (10-degree cephalad view) optimizes the acromioclavicular joint region.

J. T. Bencardino (ed.), *The Shoulder*, https://doi.org/10.1007/978-3-030-06240-8_9

When evaluating complex or comminuted fractures, CT is optimal for assessment of displacement, angulation, and injury to the adjacent neurovascular structures. In general, thin-section protocols are recommended. MRI is occasionally employed to evaluate trauma to the muscles that insert on the clavicle including the pectoralis major, deltoid, trapezius, and sternocleidomastoid muscles.

9.2.2 Clavicular Fractures

9.2.2.1 Definition

Typically, young people are at risk for clavicle fractures. Children and adolescents engage in activities that subject them to accidents and falls. In one study, falls during play or an athletic activity were the etiology of a fracture in greater than 90% of cases [2]. The point of the shoulder was usually the site of impact. Additional mechanisms of injury include direct impaction on the clavicle from assault or motor vehicle accidents and rarely a fall on an outstretched hand. Birth trauma may place excessive pressure of the shoulder against the maternal symphysis pubis producing a characteristic fracture at the junction of the middle and lateral thirds of the bone [3].

9.2.2.2 Radiographic and CT Findings

The Allman classification divides the clavicle into thirds [4]. About 80% of clavicle fractures involve the middle third of the bone (Fig. 9.1). The majority of fractures are simple and transversely oriented; however, comminuted fractures associated with butterfly fragments are not uncommon. In children, fractures may be either a greenstick or bowing-type injury. Angulation and displacement occur from the pull of the sternocleidomastoid muscle on the medial fragment and depression of the lateral fragment from the weight of the arm [5]. The degree of displacement is usually more conspicuous on the serendipity or Zanca view than on the AP view (Fig. 9.1). When a fracture is severely comminuted, CT may be indicated to assess for a concomitant injury to the subclavian artery, particularly in the setting of a rapidly growing hematoma, or to the subclavian vein and brachial plexus (Fig. 9.2).

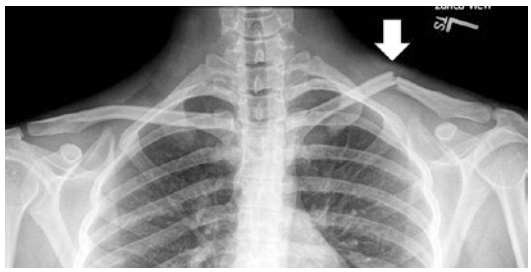

Fig. 9.1 Clavicle fracture, nondisplaced. The majority of clavicle fractures involve the middle one-third of the clavicle (arrow). Imaging both clavicles with 10° of cephalad angulation optimizes assessment of the angular deformity

Lateral third fractures account for 15% of clavicle fractures (Fig. 9.3) [6]. The Neer classification is dependent on the location of the fracture with respect to the coracoclavicular (CC) ligament which consists of a conoid (medial) and trapezoid (lateral) component. A type 1 fracture is located lateral to the CC ligament and has minimal displacement. A type 2a fracture occurs medial to the conoid component where a type 2b occurs between the fibers of the CC ligament, disrupting the conoid component. Type 2 injuries can lead to significant separation between the coracoid process and the clavicle. Because it has the highest risk for nonunion, it generally requires surgical fixation. A type 3 fracture is intra-articular, thus predisposing to arthritis. A type 4 fracture occurs in pediatric patients with the displacement at the junction of the metaphysis and the growth plate. A type 5 fracture is comminuted but contains a small inferior fragment that remains attached to the CC ligament and is similar to a type 2 variant.

Less than 5% of clavicle fractures involve the medial third (Fig. 9.4). These are difficult to visualize if not displaced owing to the overlap of the ribs and spine. Since these fractures are caused by direct trauma, CT is useful to further characterize the fracture to assess the surrounding structures and to evaluate the sternoclavicular joint. There are two types: transverse fractures and intra-articular fractures.

9.2.2.3 Ultrasound Findings

Currently, sonography is not routinely used in adults with clavicle fractures except to diagnose vascular complications such as a pseudoaneurysm or the formation of a hematoma. Sonography, however, is commonly utilized in neonates to visualize clavicular birth fractures [7].

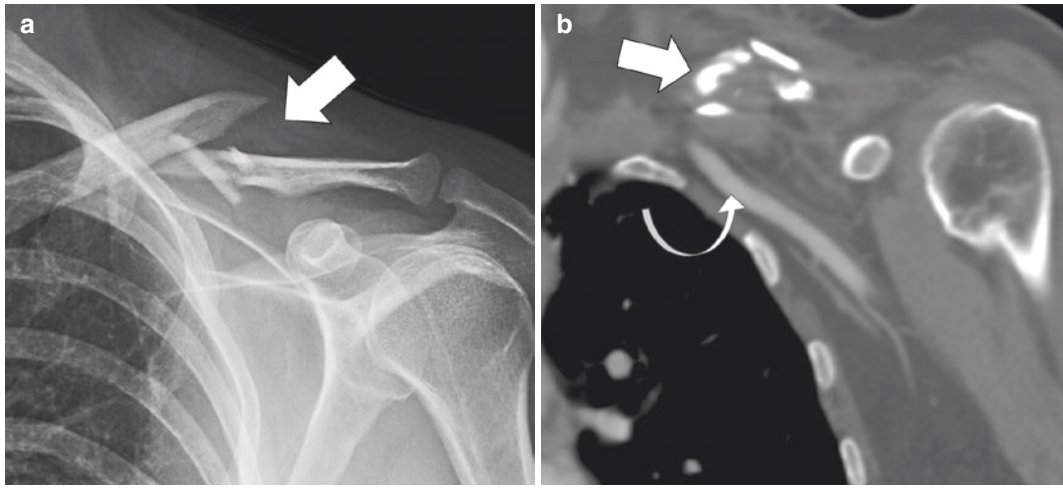

Fig. 9.2 Clavicle fracture, comminuted. (**a**) A comminuted mid-clavicular fracture (arrow) is frequently displaced from the pull of the sternocleidomastoid muscle on the medial fragment while the weight of the arm depresses the lateral fragment. (**b**) CT is recommended when there is significant displacement of the clavicle fragments (arrow) to evaluate the vascular structures (curved arrow) and the brachial plexus

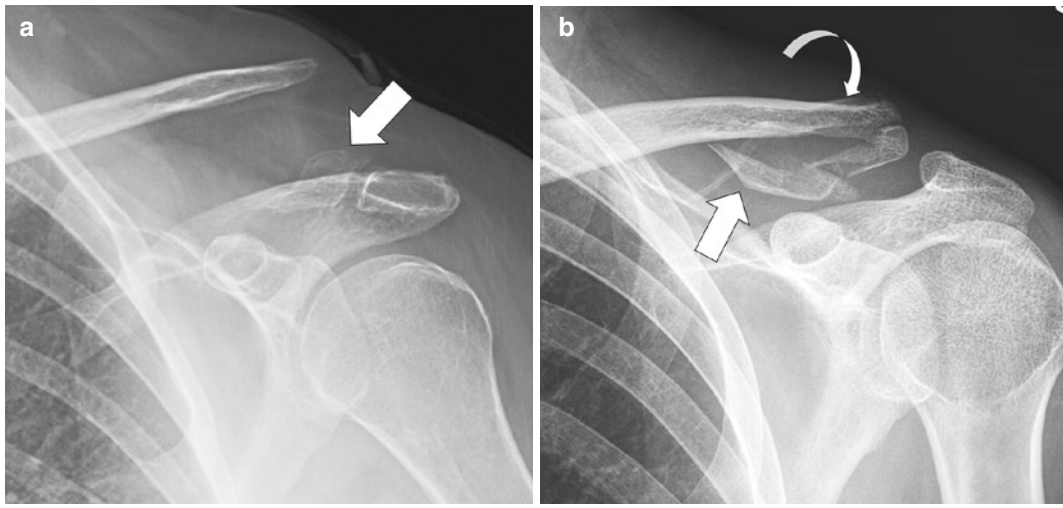

Fig. 9.3 Distal clavicular fractures. (**a**) This patient had a Neer type 2 fracture occurring medial to the coracoclavicular (CC) ligament, resulting in a fragment in anatomic alignment with the acromioclavicular (AC) joint (arrow) and marked superior migration of the rest of the clavicle from the coracoid process. (**b**) A different patient with a type 5 fracture with an inferior fragment still attached to the CC ligament, another fragment attached to the AC joint, and the rest of the clavicle (curved arrow) displacing superiorly

9.2.2.4 MR Findings

On occasion, MRI may be used to evaluate a clavicle fracture when there is a simultaneous muscle injury or accumulation of a pathologic fluid collection. When the soft tissues protrude above the clavicle or into the axilla, for example, it may be an indication that there is an enlarging hematoma from an occult vascular injury.

9.2.3 Postoperative Imaging

Most clavicular fractures heal without sequela although a nonunion occurs in 1–4% of patients [8]. When fixation is required, radiographic follow-up is sufficient with standard clavicle projections. There are two common fixation techniques employed. For midshaft fractures, uni-cortical

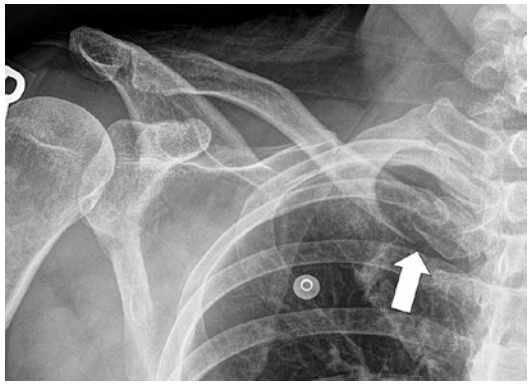

Fig. 9.4 Medial clavicle fracture. Fractures involving the medial clavicle (arrow) are uncommon but are frequently overlooked owing to the overlap of the spine and ribs

plate fixation is common with the plate on the superior cortical margin with screws directed inferiorly in order to avoid the neurovascular structures [9]. For distal type 2 clavicle fractures, it is not uncommon to see a variation of a clavicle hook plate that has an S-shaped contour so that the lateral end can be placed underneath the inferior margin of the acromion process [10].

9.3 Sternoclavicular Joint

9.3.1 Pertinent Imaging Findings

The sternoclavicular (SC) joint is a di-arthrodial joint at the medial end of the clavicle. The disc within the SC joint divides the gliding synovial joint into medial and lateral compartments. Supporting the joint are the interclavicular, costoclavicular, anterior sternoclavicular, and posterior sternoclavicular ligaments. Radiographic evaluation consists of a PA view of both SC joints with the beam centered over the manubrium, and bilateral PA oblique projections. It is important to confirm symmetric position of the clavicular head and when in doubt CT is confirmatory. The rhomboid fossa is a variant that occurs in the inferomedial aspect of the clavicle corresponding to the insertion of the costoclavicular ligament. It is depicted by an irregular concavity located lateral to the head of the clavicle and is seen commonly in males.

9.3.2 Sternoclavicular Joint Injuries

9.3.2.1 Definition

Dislocation of the SC joint is uncommon accounting for 2–3% of all shoulder girdle dislocations [11]. Anterior dislocations are overwhelmingly more common than posterior dislocations but the latter type can be more severe because of associated injuries to adjacent structures. The mechanism of injury for anterior dislocations is most often indirect trauma with impaction to the anterior shoulder with the clavicle acting as a fulcrum. Posterior dislocation usually occurs as a result of a direct blow against the medial clavicle. Complete disruption of the SC joint may result in scapulothoracic dissociation.

9.3.2.2 Radiographic and CT Findings

Diagnosis of a SC joint dislocation is challenging on AP radiographs and this abnormality is frequently missed on initial inspection. Detection requires asymmetry of the joint space which may not be evident with minor subluxation unless there is also superior subluxation (Fig. 9.5). The Allman classification defines three types [3]. In a type 1 dislocation, there is partial disruption of the SC ligaments. In type 2, there is complete rupture of the SC ligaments. In type 3, the SC ligaments and the costoclavicular ligament are torn.

The modality of choice for confirmation is CT. Rapidly acquired images display the direction of the dislocation, degree of osseous displacement, presence of any associated fracture, as well as any potential complication to the adjacent structures such as the great vessels. Approximately 25% of posterior dislocations are associated with a laceration of the superior vena cava, thoracic outlet syndrome from venous compression, compression of the recurrent laryngeal nerve, pneumothorax or pneumomediastinum from esophageal or tracheal rupture, or injury to the subclavian or carotid artery [12].

9.3.2.3 Ultrasound Findings

Ultrasound has been described as a potential screening tool to assess possible sternoclavicular dislocation [13].

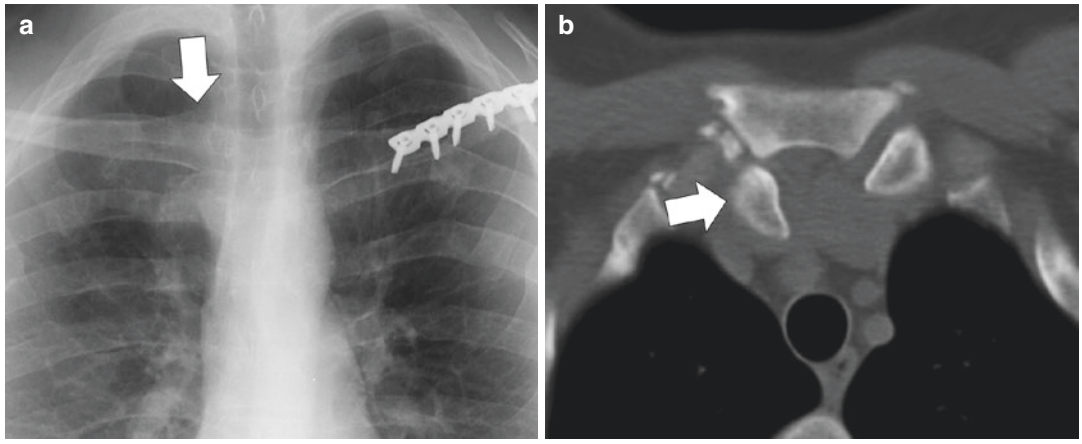

Fig. 9.5 Sternoclavicular joint (SC) separation. (**a**) Frontal radiograph of the chest shows asymmetric elevation of the right clavicular head (arrow) compared to the left. (**b**) Axial CT image shows that the asymmetry is caused by posterior dislocation of the right clavicular head (arrow). When this occurs, it is important to thoroughly evaluate the vascular structures

9.3.2.4 MR Findings

The multiplanar capabilities of MRI along with its superior soft tissue resolution have made this modality particularly effective for characterizing ligamentous tears and cartilaginous injuries [14]. MR angiography is very helpful in elucidating occult vascular injury as well.

9.3.3 Postoperative Imaging

The treatment of choice for SC dislocations is closed reduction and immobilization of the arm with a sling [15]. Delay in diagnosis may lead to instability; stabilization procedures of the SC joint with a trans-osseous tension band or ligamentous reconstruction are potential long-term solutions. However, in some patients, resection arthroplasty of the medial end of the clavicle is the only option for treating persistently painful SC joints.

9.4 Acromioclavicular Joint

9.4.1 Pertinent Imaging Findings

The acromioclavicular (AC) joint is a diarthrodial gliding joint at the lateral end of the clavicle containing a variably developed intra-articular disc. This synovial joint is supported by the capsule, the AC ligaments, and the CC ligament. Radiographic evaluation consists of an AP view of the upper thorax including AC joints and a 15-degree cephalad-angled view and symmetry with the contralateral joint is a key observation. If findings are equivocal or surgery is contemplated, bilateral weight-bearing stress views may be performed to confirm the severity of pathology. The normal width of the AC joint is 2–6 mm and it decreases with age [16]. Any discrepancy of the CC distance greater than 3–4 mm, or asymmetry of the AC joint space greater than 2 mm, may indicate a rupture of the CC ligament. An axillary view is useful especially when there is concern of a posterior subluxation. Though not routinely used, MRI is an excellent modality that enables comprehensive evaluation of the osseous structures and soft-tissue stabilizers of this joint.

9.4.2 Acromioclavicular Joint Injuries

9.4.2.1 Definition

The AC joint is the second most commonly dislocated joint in the shoulder accounting for about

12% of all shoulder dislocations [17]. Two injury mechanisms are responsible, either a direct fall on the shoulder or a fall on an outstretched hand. The force applied determines the spectrum of pathology. The initial injury is a strain of the AC ligaments. As the force increases, the trapezoid component of the CC ligament ruptures then followed by the conoid component as the force is increased. With complete rupture of the CC ligament, the clavicle is allowed to detach resulting in injuries to the insertion of the deltoid and trapezius muscles.

9.4.2.2 Radiographic and CT Findings

A six-point grading system is used to classify and treat AC joint injuries [18]. A grade 1 separation indicates stretching of the AC ligaments without capsular disruption. Radiographs appear normal or may show mild soft-tissue swelling over the joint. A grade 2 separation results in disruption of the AC ligaments and an incomplete tear of the CC ligament (Fig. 9.6). The clavicle elevates superiorly but usually less than 50% of the width of the clavicle and the AC joint widens compared to the contralateral joint, particularly with weight-bearing views. A grade 3 separation is a true dislocation with complete rupture of the AC and CC ligaments (Fig. 9.7). A variation can occur in people younger than 25 years of age depicted by an avulsion fracture at the base of the coracoid process but with an intact CC ligament.

The three latter grades are uncommon. In grade 4 injuries, the clavicle displaces posteriorly into or through the trapezius muscle. In grade 5 injuries, elevation of the clavicle is more severe than in a grade 3 separation. In grade 6 injuries, the clavicle dislocates inferiorly below the coracoid or acromion process often occurring with associated rib fractures.

9.4.2.3 Ultrasound Findings

Ultrasound may be used to screen for AC joint separation but it is suggested only if CT or MRI is not available.

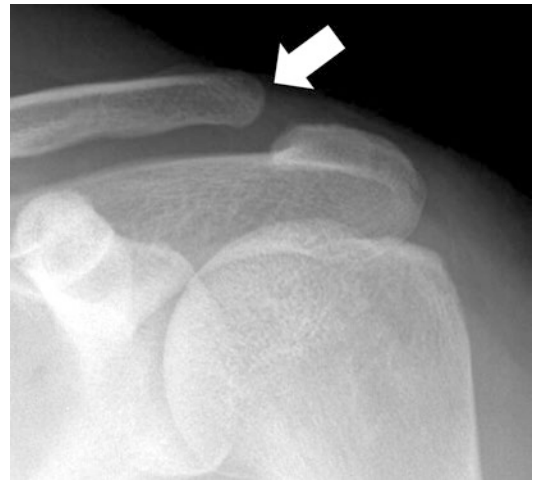

Fig. 9.6 Acromioclavicular (AC) joint separation, type 2. The distal clavicle (arrow) elevates superiorly by about half of the shaft width relative to the acromion process owing to a rupture of the AC ligament and partial tears of the coracoclavicular ligaments

9.4.2.4 MR Findings

MRI is a useful tool for assessment of AC joint pain and it has recently been advocated for evaluation of acute AC joint separations [19]. The main limitation of radiography is accuracy in the categorization of the injury and this may have an effect on the treatment. MR enables distinction between grade 2 and 3 injuries and also has been shown to reclassify radiographic grading to a lesser type in as many as 36% of patients and to a more severe type in greater than 11% of patients [20].

9.4.3 Postoperative Imaging

There are several surgical options in the management of AC joint dislocations [21, 22]. Current evidence suggests that operative management of type 3 fractures has better results. Early surgery has been reported to have better cosmetic and radiologic outcomes and a lower risk for infection, and reduce the overall incidence of failed surgery.

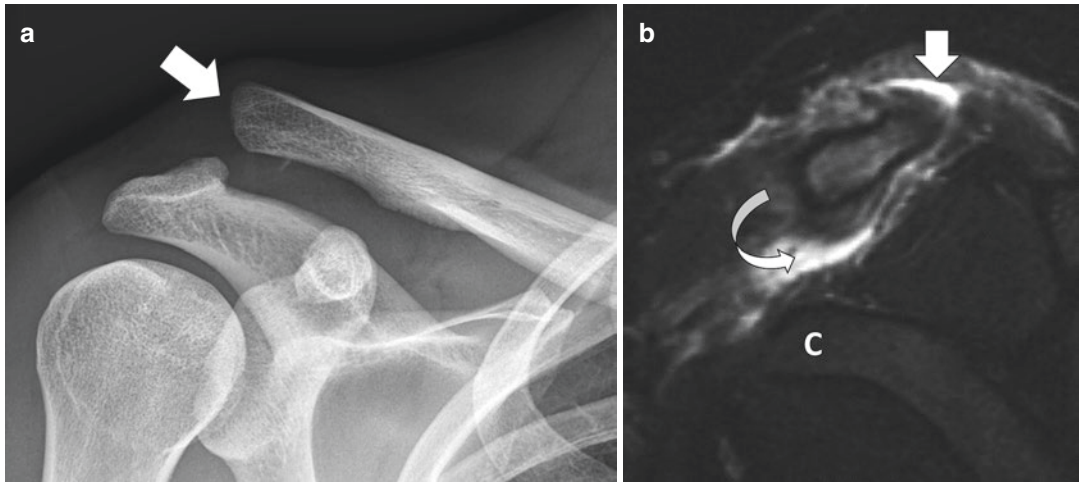

Fig. 9.7 Acromioclavicular (AC) joint separation, type 3. (**a**) Frontal radiograph shows complete disarticulation of the clavicle (arrow) from the acromion process and an abnormally wide distance between the clavicle and the coracoid process. (**b**) Sagittal T2-weighted MR image shows complete disruption of the coracoclavicular ligaments (curved arrow) and a hematoma (arrow) where the superior AC ligament is typically visualized. [C—coracoid]

9.5 Scapula

9.5.1 Pertinent Imaging Findings

The scapula is a large, triangular flat bone located in the dorsolateral aspect of the thorax that is almost entirely surrounded by muscles. Because the body of the scapula is anteverted 30–40° with respect to the coronal plane of the body, a true AP view of the scapula is actually an AP oblique radiograph of the shoulder. This projection allows visualization of the superior and inferior angles in the medial aspect of the blade, the superior and lateral borders, the tip of the coracoid process, the majority of the spine, the portion of the acromion that articulates with the clavicle, and the glenoid neck and fossa. A lateral projection, or Y-view, allows assessment of the body, acromion, and base of the spine. An axillary view depicts the acromion and coracoid processes as well as the glenoid fossa and neck. CT, on the other hand, is preferred when there is a complex fracture of the scapula particularly when performed with 3D reconstruction.

Ossification centers have a typical radiographic appearance and should not be mistaken for a fracture. An os acromiale represents failure of fusion of an apophysis (which generally occurs by 25 years of age) appearing as a transverse lucency. It is common and occurs in 7–10% of people [23]. True fractures of the acromion process usually occur at the junction of the spine and the acromion. One pitfall is a chronic fracture with nonunion which may be impossible to differentiate from a basi-acromial type of os acromiale unless there are comparison radiographs.

9.5.2 Scapular Fractures

9.5.2.1 Definition

Scapular fractures account for 3–5% of fractures in the shoulder girdle [24]. Fractures of the scapula require major trauma with either axial loading on an outstretched arm or direct forces aimed at the scapula such as those that occur from a fall from a height, motor vehicular trauma, or crushing injury. Fractures of the glenoid rim and coracoid process may also occur with glenohumeral joint dislocations. There are numerous classification systems for describing scapular fractures but none predominate; thus, fractures often are described according to the anatomic area involved including the acromion process, coracoid process,

scapular neck, and glenoid fossa/rim with the latter subdivided into extra- and intra-articular types. The majority of fractures involve the body and inferior glenoid neck and over 20% enters the spinoglenoid notch [25].

9.5.2.2 Radiographic and CT Findings

Fractures of the body constitute the most common fracture of the scapula. The Grashey and lateral projections are useful since these fractures, though often comminuted, have conspicuous vertical and/or horizontal components. Fractures through the scapular neck are frequently displaced and are unstable if the clavicle and CC ligament are also disrupted.

Coracoid fractures are categorized according to where the fracture is located with respect to the CC ligament attachment (Fig. 9.8). A type 1 fracture occurs proximal to the CC ligament and may be associated with AC joint separation, fractures of the clavicle, and/or other scapular fractures involving the superior scapula and glenoid [26]. A type 2 fracture occurs distal to the CC ligament. Acromion process fractures are usually transversely oriented at its base. Three types have been described by Kuhn et al. A type 1 fracture is not displaced and has two subtypes: avulsive type 1a and impactive type 1b. A type 2 fracture is displaced but does not encroach on the subacromial space. A type 3 fracture is either inferiorly displaced or associated with a superiorly displaced glenoid fracture. Coracoid and acromion fractures may be radiographically occult or difficult to visualize. Axillary views and trans-scapular Y views are considered essential projections for depicting fractures of either bony tubercle.

Glenoid fractures are categorized as either extra-articular or intra-articular [27]. In extra-articular fractures, the integrity of the clavicle and AC joint is important (Fig. 9.9). Intra-articular fractures comprise about 10% of scapular fractures and is most commonly classified according to the classification described by Ideberg (Fig. 9.10) [28]. Type 1a is most common and represents an anterior chip fracture of the glenoid rim. Type 1b is through the posterior glenoid rim. Type 2 is a transverse or an oblique fracture through the inferior glenoid fossa with inferior displacement. Type 3 is a transverse fracture through the superior glenoid fossa and extending to the superior border. Type 4 is a transverse fracture through the body extending to

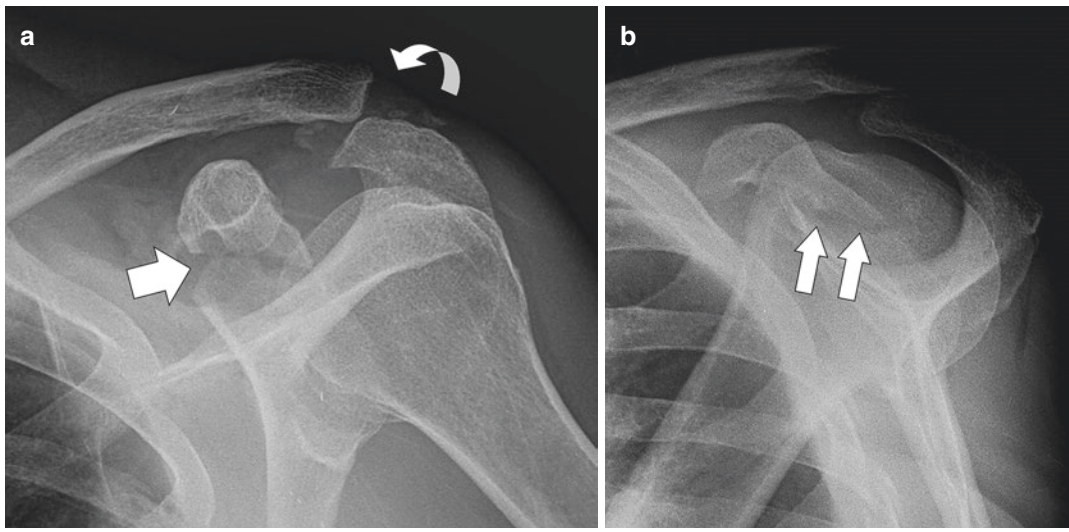

Fig. 9.8 Coracoid fracture, type 1. (**a**) Frontal radiograph shows cortical disruption near the base of the coracoid process (arrow). There is also a type 3 AC separation (curved arrow). (**b**) The scapular Y-view offers a second opportunity to observe this fracture (arrows) since it is often obscured in the frontal projection owing to bony overlap

Fig. 9.9 Scapular fracture, extra-articular type. Extra-articular fractures (arrows) are frequently associated with concomitant injuries of the clavicle (curved arrow) and acromioclavicular joint

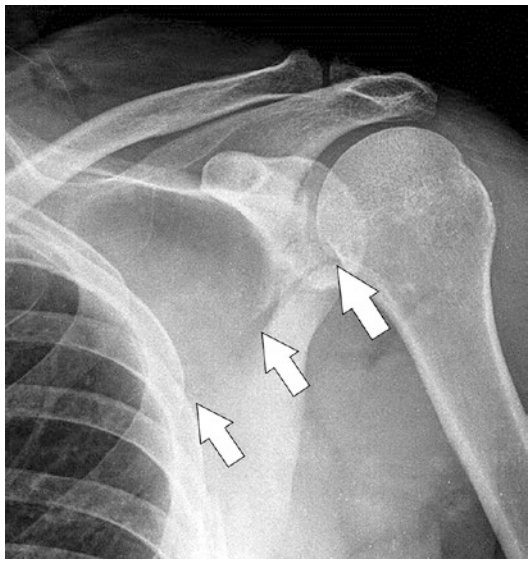

Fig. 9.10 Scapular fracture, intra-articular type. Fractures that involve the glenoid fossa and rim are considered intra-articular. The location of the fracture in the fossa is useful for its characterization. This patient has an Ideberg type 4 fracture extending from the fossa to the medial border

the medial border. Type 5 is a type 4 with separation of the glenoid. Type 6 is a comminuted fracture.

Approximately 25–43% of scapular fractures are not detected initially [29]. Scapular fractures are frequently associated with other injuries to the rib, clavicle, spine, extremities, lung, vascular structures, and brachial plexus or central nervous system. These injuries have been reported in 81–98% of scapular fractures [24, 30]. 3DCT is optimal for evaluating these fractures since it reliably identifies extension to the superior, medial, and lateral borders which are clinically relevant [31].

9.5.2.3 Ultrasound Findings

Ultrasound has been useful for diagnosing occult coracoid fractures but otherwise is not generally employed for assessment of this bone [32].

9.5.2.4 MR Findings

MRI allows simultaneous inspection of the bone and the ligaments of the shoulder girdle but is best reserved as a follow-up study after the osseous injuries have been ascertained acutely. It is useful for the evaluation of compartment syndrome of the scapula.

9.5.3 Postoperative Imaging

The majority of scapular fractures are treated conservatively but because closed reduction is not possible malalignment is a common outcome. Intra-articular fractures that are complex do well with surgery [33, 34]. The goal is to restore stability to the glenoid when fractures are displaced more than 1 cm or more than 25% of the articular surface is involved. Scapular neck fractures may be repaired if medially displaced more than 1 cm or angulated more than 40°.

9.6 Glenohumeral Joint

9.6.1 Pertinent Imaging Findings

The glenohumeral joint is a spheroidal joint that has the distinction of being the most mobile articulation in the body. The range of motion afforded by this joint is related to the disproportionate

sizes of the articulating surfaces and the relative lack of osseous constriction. What this joint has in mobility, however, it lacks in stability. It is the most commonly dislocated joint in the skeleton with 50% of dislocations affecting this articulation [35]. Reportedly, shoulder dislocations occur at a rate of 1–2% in the general population and have an incidence of as high as 7% in selected groups of athletes [36]. Anterior dislocations are most common. Posterior dislocations are often difficult to diagnose. Inferior dislocations, referred to as luxatio erecta, are caused by either hyperabduction of the arm or a direct blow against the length of the arm with the shoulder maximally abducted. Superior dislocations are rare and caused by forces directed cephalad along an adducted arm.

Evaluation of trauma usually begins with a three- or four-view radiographic series that include an AP, oblique AP (Grashey), lateral Y, and axillary projections. It is generally recommended that the AP view be performed with the arm in neutral position or internally rotated, and the Grashey view be performed with the humerus externally rotated to allow a more complete depiction of the humeral head. Internal rotation depicts the anterior and posterior articular surfaces and brings the lesser tuberosity cortex into profile. External rotation, on the other hand, brings the greater tuberosity into full profile and enables much of the medial articular surface to be visualized. An advantage of the Grashey view over the AP shoulder projection is that it eliminates the overlap of the glenoid rim and the humeral joint. The nearly spherical head articulates with the glenoid fossa much like a golf ball sitting on a tee. The axial view is optimal in showing subtle decentering of the humerus that may not be detectable on other radiographic projections and to depict hypertrophic osseous changes in the glenoid rim that may herald an underlying labral abnormality.

When there is an injury of the glenohumeral joint, CT is an excellent imaging tool for further characterizing the humeral head and glenoid. However, it does not show the connective and cartilaginous tissues as well as MRI, even in the setting of arthrography. When MRI is necessary, it can depict injuries involving the joint capsule, labrum, articular cartilage, tendons and supporting ligaments, as well as marrow edema that are associated with bone contusions and occult fractures.

9.6.2 Anterior Glenohumeral Joint Dislocation

9.6.2.1 Definition

Anterior dislocation accounts for about 95% of all glenohumeral joint dislocations. Four types of anterior dislocations have been described depending on the location of the humeral head after it has become dislocated: subcoracoid, subclavicular, subacromial, and intrathoracic. The majority of anterior dislocations are caused by abduction with forced external rotation of the arm, although a direct blow to the back of the shoulder may be an occasional cause [37].

9.6.2.2 Radiographic and CT Findings

Radiographic diagnosis of an anterior dislocation is not difficult. The most common type of anterior dislocation is a subcoracoid dislocation characterized by anterior, inferior, and medial displacement of the humeral head beneath the coracoid process (Fig. 9.11). A subglenoid dislocation is characterized by anterior, inferior, and more medial displacement of the humeral head so that it comes to rest beneath the inferior rim of the glenoid. A subclavicular dislocation results in anterior, inferior, and even more medial displacement so that the humeral head terminates beneath the clavicle. Lastly, an intrathoracic anterior dislocation occurs when the humeral head penetrates an intercostal space.

The shoulder girdle must be scrutinized for certain injuries after a dislocation. A Hill-Sachs lesion, an impaction fracture of the posterolateral aspect of the humeral head, occurs when the humeral head becomes perched against the inferior aspect of the anterior glenoid rim [38]. It is detectable as a wedge-shaped or concave defect in the posterolateral aspect of the head when it is internally rotated. It is best depicted on an AP shoulder view but a Stryker notch view is also

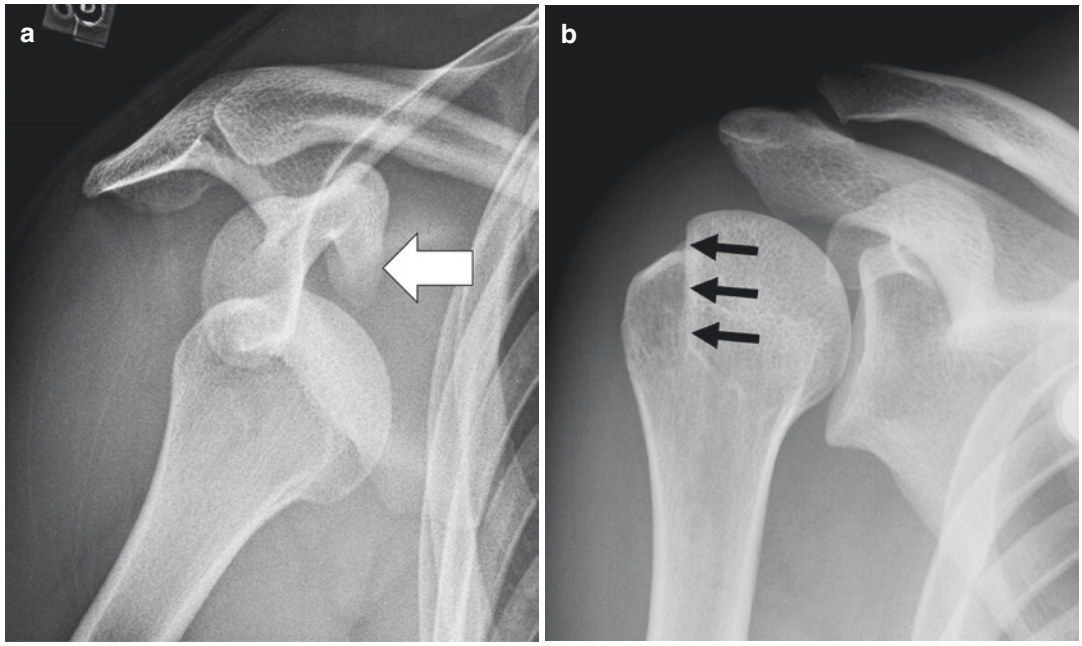

Fig. 9.11 Anterior glenohumeral joint dislocation. (**a**) The humeral head has dislocated anteriorly from the glenoid fossa and is located beneath the coracoid process (arrow). The subcoracoid type of anterior dislocation is the most common type. (**b**) After reduction, a sclerotic linear abnormality (arrows) seen on an internally rotated view of the humerus defines the posteromedial border of the Hill-Sachs lesion

useful. If the defect is sufficiently large, a linear sclerotic band may be seen vertically oriented on the head which defines the posterior edge of the impaction fracture. CT is reliable for diagnosis and characterization. A Hill-Sachs lesion is differentiated from the normal trough by its more superior location [39].

In about 8% of patients, a concomitant fracture of the anteroinferior glenoid rim (osseous Bankart lesion) occurs but the reported incidence has been as high as 31% (Fig. 9.12) [40]. Close scrutiny on AP and lateral radiographs is required since the fragment of bone may be quite small but a well-positioned lateral view is most optimal. An uncommon avulsion fracture may occur at the humeral attachment of the inferior glenohumeral ligament referred to as a BHAGL (bony humeral avulsion of the glenohumeral ligament) lesion (Fig. 9.13). An osteochondral defect of the glenoid has also been associated with anterior dislocations and is usually occult unless large [41].

About 15–25% of anterior dislocations are associated with a fracture of the greater tuberosity which can be displaced or comminuted (Fig. 9.14) [40]. Another 2% of dislocations are associated with a fracture of the surgical neck of the humerus, scapular body, acromion process, and clavicle.

9.6.2.3 Ultrasound Findings

Sonography is a useful modality for evaluating the rotator cuff in patients with shoulder instability and for identifying Hill-Sachs lesions but is overall inferior to MRI for characterization of osseous lesions, capsular and ligamentous injuries, and labral tears [42, 43].

9.6.2.4 MR Findings

MRI has become indispensable for the evaluation of shoulder instability [44]. Acute dislocations are characterized by bone marrow edema surrounding a Hill-Sachs lesion and in the anterior glenoid rim as well. Pathologic entities that are occult or not easily seen on radiographs or CT include avulsions and tears of the subscapularis tendon, stripping of the capsule, and soft-tissue Bankart

Fig. 9.12 Osseous Bankart lesion. There is a displaced fragment of bone arising from the anteromedial aspect of the glenoid rim (arrow). The size of the fragment correlates with the degree of instability and if more than 25% of the articular surface is involved surgical repair with the Latarjet-Bristow (coracoid transfer) procedure

Fig. 9.14 Anterior shoulder dislocation with greater tuberosity fracture. As the humeral head dislocates anteriorly, the force of impaction against the anterior glenoid rim can produce a fracture through the greater tuberosity (arrow) which often is displaced or comminuted

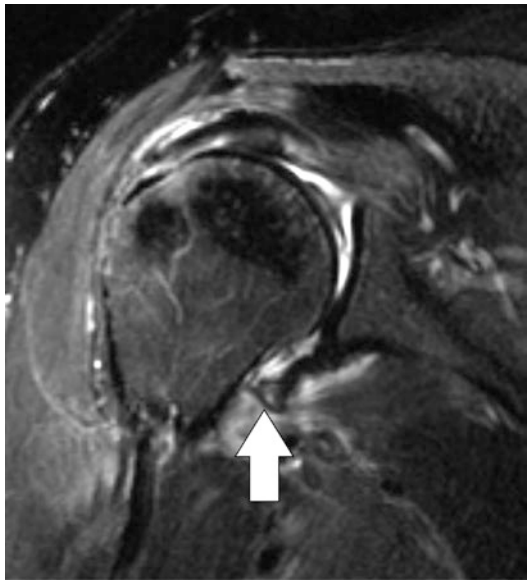

Fig. 9.13 Bony humeral avulsion of the glenohumeral ligament (BHAGL) lesion. Coronal T2-weighted MR image shows an avulsed fragment of bone (arrow) arising from the humeral attachment of the anterior band of the inferior glenohumeral ligament. This lesion may mimic an osseous Bankart lesion on radiographs

lesions, defined as an avulsion of the anterior labrum by the anterior band of the inferior glenohumeral ligament associated with disruption of the anterior periosteum. Bankart variants with the acronyms HAGL, ALPSA (anterior labroligamentous periosteal sleeve avulsion), and GLAD (glenoid labral articular disruption) lesions are best characterized with MR arthrography [45].

9.6.3 Posterior Glenohumeral Joint Dislocation

9.6.3.1 Definition

Posterior dislocations are much less common than anterior dislocations accounting for less than 5% of glenohumeral dislocations [46]. The mechanism of injury is either a fall on an outstretched hand or a direct trauma to a flexed, adducted, and internally rotated shoulder which forces the humeral head posteriorly. There are three types of posterior shoulder dislocations. Nearly all, about 98%, are the subacromial type.

The posterior subglenoid and subspinous types are uncommon. Bilateral dislocations are typically associated with seizures.

9.6.3.2 Radiographic and CT Findings

The radiographic features of posterior dislocations often are subtle so that over one-half of dislocations are still missed on initial inspection [47]. When the humeral head dislocates posteriorly, the stretched anterior musculature pulls it back forcing it to impact against the posterior glenoid rim. This creates a wedge-shaped impaction, referred to as a trough lesion, in the anteromedial aspect of the humeral head that is similar to a Hill-Sachs lesion (Fig. 9.15) [48]. It appears as a vertically oriented dense linear band that parallels the medial cortex of the humeral head on internally rotated frontal radiographs of the shoulder. An axillary view is useful in characterizing the size of the lesion. The incidence of a trough lesion has been estimated to occur in 29–75% of all dislocations [48, 49]. Reverse osseous Bankart lesions are generally difficult to detect radiographically and usually require CT for confirmation (Fig. 9.16).

There are several important radiographic signs that are associated with posterior shoulder dislocations [50]. These radiographic observations underscore the difficulty in making this diagnosis (Fig. 9.17). The *lightbulb* sign is a persistently internally rotated arm on all views of a shoulder series when the head is perched on the glenoid. The *rim* sign indicates a widened glenohumeral joint exceeding 6 mm in width. The *crescent* (absent half-moon) sign is absence of the normal overlap between the glenoid and humeral head. A disrupted scapulohumeral arch indicates humeral head subluxation.

A lesser tuberosity fracture (25% incidence) (Fig. 9.18) and humeral head fracture (10% incidence) are two additional observations that should elicit a search for other indicators of a posterior dislocation [48].

9.6.3.3 Ultrasound Findings

Sonography has a limited role in patients with acute posterior shoulder instability.

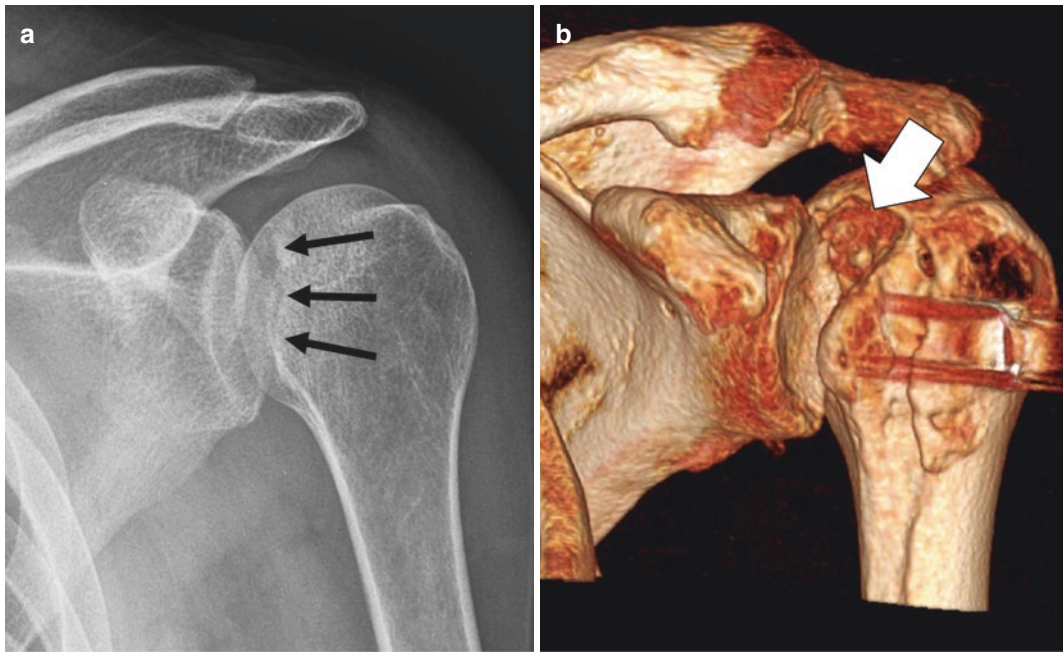

Fig. 9.15 Trough lesions in posterior glenohumeral joint dislocations. (**a**) This patient shows a posteriorly dislocated humerus with an impaction fracture in the anterior surface of the humeral head manifested as a linear vertically oriented area of sclerosis (arrows). (**b**) A 3D CT image in another patient shows the effect of a chronic dislocation with the formation of a pseudoarthrosis with widening of the trough lesion (arrow) as it toggles on the posterior glenoid rim

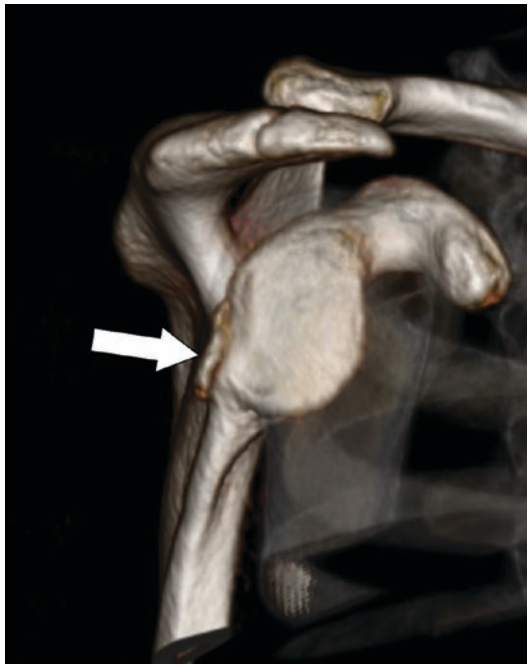

Fig. 9.16 Reverse osseous Bankart lesion. A disarticulated 3D CT image of the scapula shows a fracture of the posterior glenoid rim with a displaced fragment (arrow) in a patient who had sustained a posterior glenohumeral joint dislocation

9.6.3.4 MR Findings

The presence of bone marrow edema in the anterior humeral head is consistent with an acute impaction injury [51]. A reverse soft-tissue Bankart lesion represents damage to the posterior labrum that occurs either when the humeral head displaces posteriorly or when it impacts the posterior glenoid rim. The labrum may appear detached or fragmented, and the capsule may be stripped or torn.

9.6.4 Postoperative Imaging

The focus of this section is treatment of fractures that have been sustained during a glenohumeral joint dislocation. 3DCT and MRI are both useful for assessing the size of glenoid and humeral defects [52, 53].

Glenoid defects that exceed 25% of the fossa usually require surgical management for best results. The Latarjet-Bristow procedure is performed in patients with large osseous Bankart fractures and has been popularized owing to excellent outcomes and a low risk for recurrence [54]. In this open surgical proce-

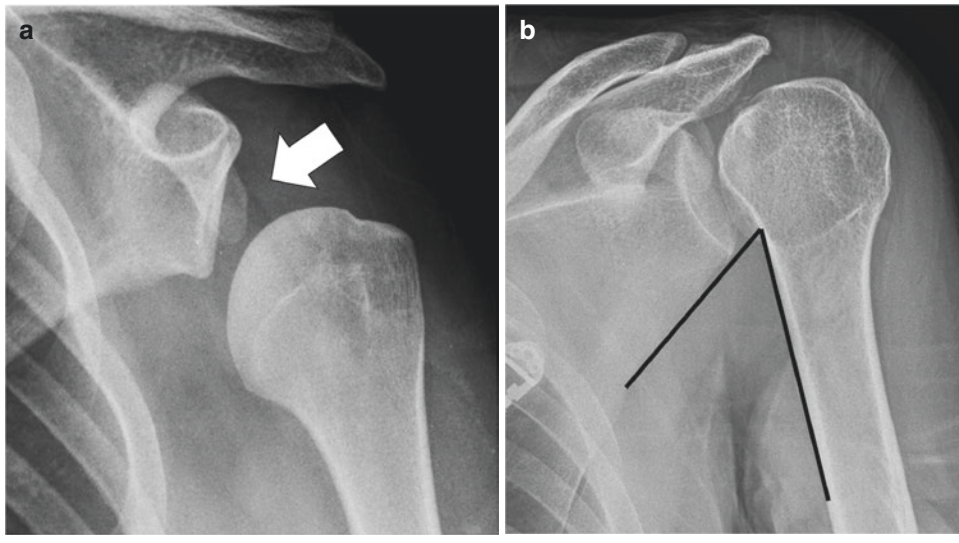

Fig. 9.17 Radiographic signs associated with a posterior shoulder dislocation. (**a**) A rim sign is present when the glenohumeral joint measures greater than 6 mm in width (arrow). The humeral head does not have to sublux inferiorly or superiorly for this sign to be present. (**b**) This scapulohumeral arch is formed by the smooth transition of the cortical margins formed by the lateral scapula, inferior glenoid neck, surgical neck of the humerus, and medial margin of the humeral shaft. In this patient, there is a break in the arch producing an angular deformity (black lines). Note that there is a rim sign as well

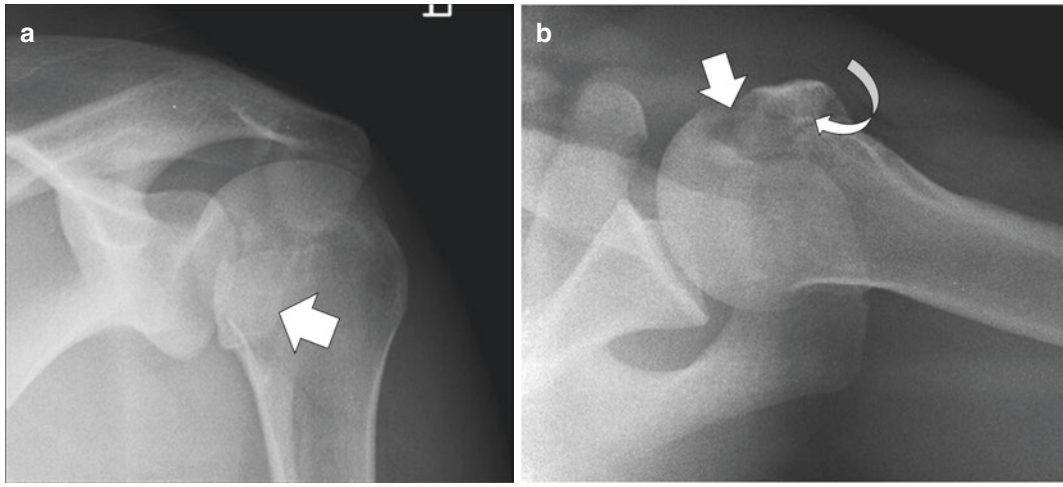

Fig. 9.18 Lesser tuberosity fracture in a posterior shoulder dislocation. (**a**) Frontal radiograph shows that the humeral head is perched against the posterior glenoid rim and there is double density seen in the region of the lesser tuberosity (arrow). (**b**) The axillary view shows a prominent trough defect (arrow) just medial to the lesser tuberosity fracture (curved arrow)

dure, a portion of the coracoid process is harvested as a bone graft and then transferred to the anterior glenoid along with the attached muscles, thus simultaneously replacing the absent bone and providing an additional muscular strut which stabilizes the anterior capsule and reinforces the subscapularis tendon. Patients with large posterior glenoid defects can be effectively treated using the McLaughlin procedure which transfers the lesser tuberosity with the attached subscapularis tendon into the defect [55].

Patients with large impaction defects of the humeral head show a dramatically lower incidence of recurrence with surgery. Several procedures have been effective including transferring the infraspinatus tendon (remplissage procedure), allograft humeral head reconstruction, and partial resurfacing arthroplasty [56]. Allograft reconstruction utilizing cryopreserved femoral head allografts or bone blocks has been performed with either anterior or posterior defects when the defect involves greater than 40% of the articular surface. In severe cases, total arthroplasty may be the option to prevent future dislocations.

9.7 Proximal Humerus

9.7.1 Pertinent Imaging Findings

In order to evaluate the humeral head and proximal shaft, shoulder radiographs performed with both internal and external rotation are necessary. The proximal humerus is divided into four anatomic regions: the head, anatomic neck, surgical neck, and greater and lesser tuberosities. When a fracture occurs in the surgical neck, the axillary view is most useful for demonstrating both angulation and displacement. Complex fractures often require additional imaging with CT to further assess fracture orientation, displacement and rotation of bone fragments, angulation, and impaction/overriding for treatment and preoperative planning. When the rotator cuff attachment is involved, MRI or ultrasound may be useful for follow-up.

9.7.2 Pathologic Conditions

9.7.2.1 Definition

People who are in their sixth and seventh decades of life are susceptible to fractures of the proximal

humerus [57]. In this age group, the most common mechanism of injury is a fall on the outstretched hand. In younger people, more severe trauma like those that occur from a motor vehicle accident is responsible for humeral fractures. The muscular insertions are noteworthy since the actions of the rotator cuff, pectoralis, latissimus dorsi, and teres major muscles can influence the degree and direction of displacement of osseous fragments.

9.7.2.2 Radiographic and CT Findings

Radiography is usually sufficient for diagnosis but CT is superior for fracture characterization particularly with 3D reconstruction. Isolated fractures of the greater (Fig. 9.19) and lesser tuberosities are uncommon and may be associated with rotator cuff insufficiency. The surgical neck is the most common location for fractures in the proximal humerus (Fig. 9.20). Frequently, these fractures are impacted and extend to the greater tuberosity. Anterior and medial displacement of the shaft may occur in about 15–20% of patients owing to the action of the pectoralis major muscle while the rest usually are not significantly displaced [58]. Fractures of the anatomic neck are less common but can be complicated by avascular necrosis from disruption of the blood supply to the humeral head.

The Neer classification is a widely used classification because it provides predictive value to treatment plans [59]. The classification takes into account the number of fragments and the degree of angulation and/or displacement, roughly following the anatomic lines of epiphyseal union. Displacement from its anatomic position by more than 1 cm or angulation by more than 45° is significant. About 80% of fractures under this classification are one-part fractures without significant displacement or angulation. Another 10% are two-part fractures with displacement of shaft anteromedially with respect to the neck. Three-part fractures constitute about 3% of fractures with displacement of the surgical neck and one of the tuberosities but as long as one of the tubercles remains attached to the humeral head, the blood supply to the head is likely to remain intact. Rotator cuff tears are common with this pattern of injury as well. About 4% of fractures are four-part fractures and osteonecrosis is a common complication.

Fig. 9.19 Avulsion fracture of the greater tuberosity. An avulsion fracture of the greater tuberosity may be subtle if not displaced. An externally rotated view that depicts the footplate is optimal. When displaced, it is important to measure the separation since displacement can contribute to rotator cuff insufficiency

9.7.2.3 Ultrasound Findings

Sonography has a role in the diagnosis of humeral fractures in the neonatal period but in adults it has limited application in osteoporotic patients and for evaluation of occult fractures of the tuberosity [60].

9.7.2.4 MR Findings

MRI is useful for further assessment of symptomatic patients with an occult proximal humeral fracture [61]. These include two important groups of patients: adolescents with Salter-Harris injuries and severely osteoporotic patients. MRI depicts areas of marrow edema and areas of disrupted trabeculation.

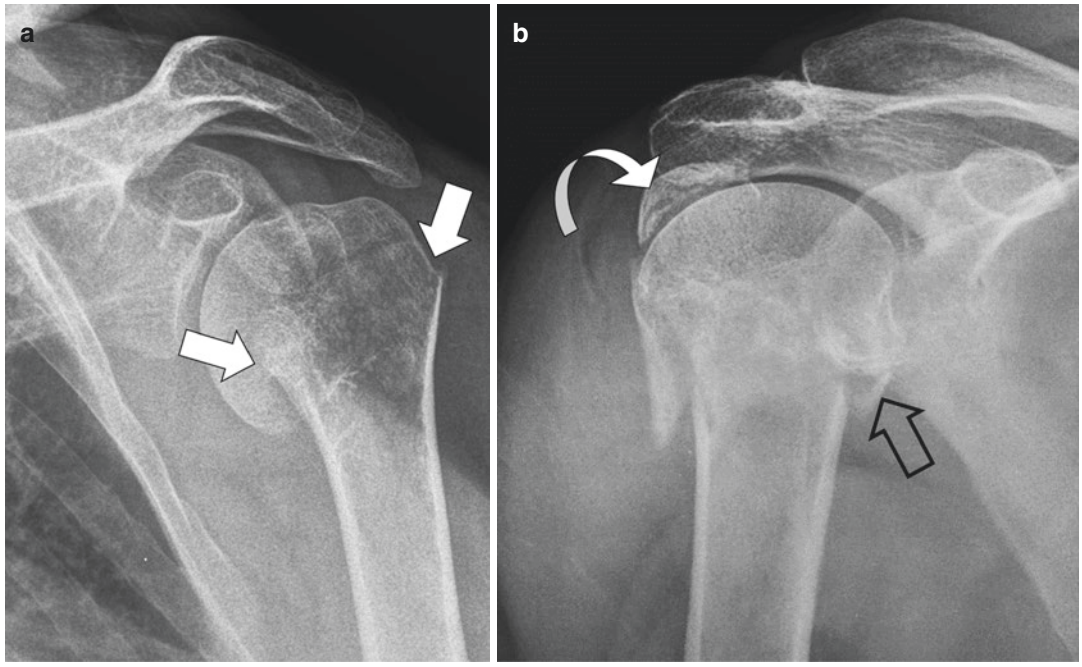

Fig. 9.20 Humerus fracture, surgical neck. (**a**) Fractures located at the surgical neck of the humerus are frequently impacted and can extend to the greater tuberosity or lesser tuberosity. (**b**) When multiple fragments are affected, the Neer classification is useful. This patient had a lesser tuberosity fracture (arrow) and a displaced greater tuberosity fragment (curved arrow), in addition to a surgical neck fracture

9.7.3 Postoperative Imaging

Radiographic findings of a greater tuberosity fractures repair is much like a rotator cuff repair. There are a variety of open reduction and internal fixation techniques using intramedullary devices for surgical neck two-part fractures. Three- and four-part fractures in elderly patients usually involve either a hemiarthroplasty, reverse shoulder arthroplasty, or complete conventional arthroplasty [62, 63].

References

1. Sheehan SE, Gaviola G, Sacks A, Gordon R, Shi LL, Smith SE. Traumatic shoulder injuries: a force mechanism analysis of complex injuries to the shoulder girdle and proximal humerus. AJR Am J Roentgenol. 2013;201:W409–24.
2. Sankarankutty M, Turner BW. Fractures of the clavicle. Injury. 1975;7:101–6.
3. Madsen ET. Fractures of the extremities in the newborn. Acta Obstet Gynecol Scand. 1955;34:41–7.
4. Allman FL. Fractures and ligamentous injuries of the clavicle and its articulations. J Bone Joint Surg Am. 1967;49:774–84.
5. Ridpath CA, Wilson AJ. Shoulder and humerus trauma. Semin Musculoskelet Radiol. 2000;4:151–70.
6. Neer CS II. Fractures of the distal third of the clavicle. Clin Orthop. 1968;58:43–50.
7. Mavrogenis AF, Mitsiokapa EA, Kanellopoulos AD, Ruggieri P, Papagelopoulos PJ. Birth fracture of the clavicle. Adv Neonatal Care. 2011;11:328–31.
8. Barger WL, Marcus RE, Ittleman FP. Late thoracic outlet syndrome secondary to pseudoarthrosis of the clavicle. J Trauma. 1984;24:847–59.
9. Donnelly TD, Macfarlane RJ, Nagy MT, Ralte P, Waseem M. Fractures of the clavicle: an overview. Open Orthop J. 2013;7:329–33.
10. Renger RJ, Roukema GR, Reurings JC, Raams PM, Font J, Verleisdonk EJ. The clavicle hook plate for Neer type II lateral clavicle fractures. J Orthop Trauma. 2009;23:570–4.
11. Sewell MD, Al-Hadithy N, Le Leu A, Lambert SM. Instability of the sternoclavicular joint: current concepts in classification, treatment and outcomes. Bone Joint J. 2013;95-B:721–31.
12. Gove N, Ebraheim NA, Glass E. Posterior sternoclavicular dislocations: a review of management and complications. Am J Orthop. 2006;35:132–6.

13. Ferri M, Finlay K, Popowich T, Jurriaans E, Friedman L. Sonographic examination of the acromioclavicular and sternoclavicular joints. J Clin Ultrasound. 2005;33:345–55.
14. Emberg LA, Potter HG. Radiographic evaluation of the acromioclavicular and sternoclavicular joints. Clin Sport Med. 2003;22:255–75.
15. Balcik BJ, Monseau AJ, Krantz W. Evaluation and treatment of sternoclavicular, clavicular, and acromioclavicular injuries. Prim Care. 2013;40:911–23.
16. Petersson CJ, Redlnd-Johnell I. Radiographic joint space in normal acromioclavicular joint. Acta Orthop Scand. 1983;54:431–3.
17. Neviaser RJ. Injuries to the clavicle and acromioclavicular joint. Orthop Clin North Am. 1987;18:433–8.
18. Melenevsky Y, Yablon CM, Ramappa A, Hochman MG. Clavicle and acromioclavicular joint injuries: a review of imaging, treatment, and complications. Skelet Radiol. 2011;40:831–42.
19. Alyas F, Curtis M, Speed C, Saifuddin A, Connell D. MR imaging appearances of acromioclavicular joint dislocation. Radiographics. 2008;28:463–79.
20. Nemec U, Oberleitner G, Nemec SF, Gruber M, Weber M, Czerny C, et al. MRI versus radiography of acromioclavicular joint dislocation. AJR Am J Roentgenol. 2011;197:968–73.
21. Modi CS, Beazley J, Zywiel MG, Lawrence TM, Veillette CJ. Controversies relating to the management of acromioclavicular joint dislocations. Bone Joint J. 2013;95-B:1595–602.
22. Babhulkar A, Pawaskar A. Acromioclavicular joint dislocations. Curr Rev Musculoskeletal Med. 2014;7:33–9.
23. Yammine K. The prevalence of os acromiale: a systematic review and meta-analysis. Clin Anat. 2014;27:610–21.
24. Imatani RJ. Fractures of the scapula: a review of 53 fractures. J Trauma. 1975;15:473–8.
25. Armitage BM, Wijdicks CA, Tarkin IS, Schroder LK, Marek DJ, Zlowodzki M, et al. Mapping of scapular fractures with three-dimensional computed tomography. J Bone Joint Surg Am. 2009;91:2222–8.
26. Ogawa K, Yoshida A, Takahashi M, Ui M. Fractures of the coracoid process. J Bone Joint Surg Br. 1997;79:17–9.
27. van Oostveen DP, Temmerman OP, Burger BJ, van Noort A, Robinson M. Glenoid fractures: a review of pathology, classification, treatment and results. Acta Orthop Belg. 2014;80:88–98.
28. Ideberg R, Grevsten S, Larsson S. Epidemiology of scapular fractures. Incidence and classification of 338 fractures. Acta Orthop Scand. 1995;66:395–7.
29. Harris RD, Harris JH. The prevalence and significance of missed scapular fractures in blunt chest trauma. AJR Am J Roentgenol. 1988;151:747–50.
30. Thompson DA, Flynn TC, Miller PW, Fischer RP. The significance of scapular fractures. J Trauma. 1985;25:974–7.
31. Audigé L, Kellam JF, Lambert S, Madsen JE, Babst R, Andermahr J, et al. The AO Foundation and Orthopaedic Trauma Association (AO/OTA) scapula fracture classification system: focus on body involvement. J Shoulder Elb Surg. 2014;23:189–96.
32. Botchu R, Lee KJ, Bianchi S. Radiographically undetected coracoid fractures diagnosed by sonography. Report of seven cases. Skelet Radiol. 2012;41:693–8.
33. Anavian J, Gauger EM, Schroder LK, Wijdicks CA, Cole PA. Surgical and functional outcomes after operative management of complex and displaced intra-articular glenoid fractures. J Bone Joint Surg Am. 2012;94:645–53.
34. Cole PA, Gauger EM, Herrera DA, Anavian J, Tarkin IS. Radiographic follow-up of 84 operatively treated scapula neck and body fractures. Injury. 2012;43:327–33.
35. Gyftopoulos S, Bencardino J, Palmer WE. MR imaging of the shoulder: first dislocation versus chronic instability. Semin Musculoskelet Radiol. 2012;16:286–95.
36. Hovelius L. Incidence of shoulder dislocation in Sweden. Clin Orthop. 1982;166:127–31.
37. Bencardino JT, Gyftopoulos S, Palmer WE. Imaging in anterior glenohumeral instability. Radiology. 2013;269:323–37.
38. Provencher MT, Frank RM, Leclere LE, Metzger PD, Ryu JJ, Bernhardson A, et al. The Hill-Sachs lesion: diagnosis, classification, and management. J Am Acad Orthop Surg. 2012;20:242–52.
39. Richards RD, Sartoris DJ, Pathria MN, Resnick D. Hill-Sachs lesion and normal humeral groove: MR imaging features allowing their differentiation. Radiology. 1994;190:665–8.
40. Kummel BM. Fractures of the glenoid causing chronic dislocation of the shoulder. Clin Orthop. 1970;69:189–91.
41. Yu JS, Greenway G, Resnick D. Osteochondral defect of the glenoid fossa: cross-sectional imaging features. Radiology. 1998;206:35–40.
42. Pavic R, Margetic P, Bensic M, Brnadic RL. Diagnostic value of US, MR and MR arthrography in shoulder instability. Injury. 2013;44(Suppl 3):S26–32.
43. Cicak N, Bilic R, Delimar D. Hill-Sachs lesion in recurrent shoulder dislocation: sonographic detection. J Ultrasound Med. 1998;17:557–60.
44. Zlatkin MB, Sanders TG. Magnetic resonance imaging of the glenoid labrum. Radiol Clin N Am. 2013;51:279–97.
45. Omoumi P, Teixeira P, Lecouvet F, Chung CB. Glenohumeral joint instability. J Magn Reson Imaging. 2011;33:2–16.
46. Shah N, Tung GA. Imaging signs of posterior glenohumeral instability. AJR Am J Roentgenol. 2009;192:730–5.
47. Arndt JH, Sears AD. Posterior dislocation of the shoulder. AJR Am J Roentgenol. 1965;94:639–45.
48. Cisternino SJ, Rogers LF, Stufflebam BC, Kruglik GD. The trough line: a radiographic sign of posterior shoulder dislocation. AJR Am J Roentgenol. 1978;130:951–4.

49. Mok DW, Fogg AJ, Hokan R, Bayley JI. The diagnostic value of arthroscopy in glenohumeral instability. J Bone Joint Surg Br. 1990;72:698–700.
50. Kowalsky MS, Levine WN. Traumatic posterior glenohumeral dislocation: classification, pathoanatomy, diagnosis, and treatment. Orthop Clin North Am. 2008;39:519–33.
51. Saupe N, White LM, Bleakney R, Schweitzer ME, Recht MP, Jost B, et al. Acute traumatic posterior shoulder dislocation: MR findings. Radiology. 2008;248:185–93.
52. Lee RK, Griffith JF, Tong MM, Sharma N, Yung P. Glenoid bone loss: assessment with MR imaging. Radiology. 2013;267:496–502.
53. Griffith JF, Yung PS, Antonio GE, Tsang PH, Ahuja AT, Chan KM. CT compared with arthroscopy in quantifying glenoid bone loss. AJR Am J Roentgenol. 2007;189:1490–3.
54. Bhatia S, Frank RM, Ghodadra NS, Hsu AR, Romeo AA, Bach BR Jr, et al. The outcomes and surgical techniques of the latarjet procedure. Arthroscopy. 2014;30:227–35.
55. Kokkalis ZT, Mavrogenis AF, Ballas EG, Papanastasiou J, Papagelopoulos PJ. Modified McLaughlin technique for neglected locked posterior dislocation of the shoulder. Orthopedics. 2013;36:e912–6.
56. Giles JW, Elkinson I, Ferreira LM, Faber KJ, Boons H, Litchfield R, et al. Moderate to large engaging Hill-Sachs defects: an in vitro biomechanical comparison of the remplissage procedure, allograft humeral head reconstruction, and partial resurfacing arthroplasty. J Shoulder Elb Surg. 2012;21:1142–51.
57. Roux A, Decroocq L, El Batti S, Bonnevialle N, Moineau G, Trojani C, et al. Epidemiology of proximal humerus fractures managed in a trauma center. Orthop Traumatol Surg Res. 2012;98:715–9.
58. Neer CS II. Displaced proximal humeral fractures. I. Classification and evaluation. J Bone Joint Surg Am. 1970;52:1077–89.
59. Neer CS II. Displaced proximal humeral fractures. II. Treatment of three-part and four-part displacement. J Bone Joint Surg Am. 1970;52:1090–103.
60. Rutten MJ, Jager GJ, de Waal Malefijt MC, Blickman JG. Double line sign: a helpful sonographic sign to detect occult fractures of the proximal humerus. Eur Radiol. 2007;17:762–7.
61. Berger PE, Ofstein RA, Jackson DW, Morrison DS, Silvino N, Amador R. MRI demonstration of radiographically occult fractures: what have we been missing? Radiographics. 1989;9:407–36.
62. Thanasas C, Kontakis G, Angoules A, Limb D, Giannoudis P. Treatment of proximal humerus fractures with locking plates: a systematic review. J Shoulder Elb Surg. 2009;18:837–44.
63. Bufquin T, Hersan A, Hubert L, Massin P. Reverse shoulder arthroplasty for the treatment of three- and four-part fractures of the proximal humerus in the elderly: a prospective review of 43 cases with a short-term follow-up. J Bone Joint Surg Br. 2007;89:516–20.